Collazo-Bigliardi, S.; Ortega-Toro, R.; Chiralt, A. (2018). Isolation and characterisation of microcrystalline cellulose and cellulose nanocrystals from coffee husk and comparative study with rice husk. Carbohydrate Polymers. 191:205-215. doi:10.1016/j.carbpol.2018.03.022

Isolation and characterisation of microcrystalline cellulose and cellulose nanocrystals from coffee husk and comparative study with rice husk

Sofía Collazo-Bigliardi[a*], Rodrigo Ortega-Toro[b] and Amparo Chiralt Boix[a]

[a]Instituto de Ingeniería de Alimentos para el Desarrollo, Universidad Politécnica de Valencia, Camino de Vera s/n, 46022 Valencia, Spain. socol@alumni.upv.es; dchiralt@tal.upv.es.

[b]Programa de Ingeniería de Alimentos, Grupo IFCRA, Facultad de Ingeniería, Universidad de Cartagena, Carrera 6 # 36-100, Cartagena de Indias D.T y C, Colombia. rortegap1@unicartagena.edu.co

*Corresponding author: Sofía Collazo-Bigliardi. Instituto de Ingeniería de Alimentos para el Desarrollo, Universidad Politécnica de Valencia, Camino de Vera s/n, 46022 Valencia, Spain. Phone: 34-963877924. Fax: 34-963877926. socol@alumni.upv.es.

Abstract

Cellulosic material from coffee husk has not been previously studied despite being a potential source of reinforcing agents for different applications. This material has been extracted and characterised from coffee husk, in parallel with previously studied rice husk. Samples have been analysed as to their ability to obtain cellulosic fibres and cellulose nanocrystals (CNC) by applying alkali and bleaching treatments and final sulphuric acid hydrolysis. Microstructural changes were analysed after treatments, and the size and aspect ratio of CNCs were determined. Crystallinity and thermal stability of both materials progressed in line with the enrichment in cellulosic compounds. The

CNC aspect ratio was higher than 10, which confers good reinforcing properties. These were tested in thermoplastic starch films, whose elastic modulus increased by 186 and 121 % when 1 wt% of CNCs from rice and coffee husks, respectively, was incorporated into the matrix. Coffee husk represents an interesting source of cellulosic reinforcing materials.

Keywords: Agro-wastes; Cellulose fibres; Cellulose nanocrystals; Biocomposite; Tensile properties.

1. Introduction

A growing concern for environmental conservation has encouraged research into the development of new types of green bio-based and biodegradable materials from natural sources for different engineering applications (Balaji, Pakalapati, Khalid, Walvekar, & Siddiqui, 2017; Bassas-Galia, Follonier, Pusnik, & Zinn, 2017; Jiang & Zhang, 2017; Brigham, 2018; Ng et al., 2015), such as biodegradable packaging materials for the food industry (Fabra, López-Rubio, & Lagarón, 2014; Talegaonkar, Sharma, Pandey, Mishra, & Wimmer, 2017). Many studies have focused on the use of agro-wastes to obtain more valuable materials in a sustainable and environmentally-friendly way, which can be applied in different industrial applications, as an alternative to conventional petroleum-derived plastics (Mondal, 2017; Reis et al., 2015). The use of residual biomass can give added value to a waste product while also offering new renewable materials. This way, lignocellulosic materials are one of the most important natural sources of renewable polymers, which are attractive because of their biodegradability, low density and excellent mechanical properties, such as great stiffness and strength (Hake, Mondal, Khan, Usmani, Bhat, & Gazal, 2017; Patel & Parsania, 2018). Several authors have studied the potential use of lignocellulosic materials as sources of reinforcing fillers for

thermoplastic biopolymers. In this sense, different agro wastes, such as sunflower stalks (Fortunati et al., 2016), hemp fibres (Luzi et al., 2016), bamboo pulp (Borkotoky, Dhar, & Katiyar, 2018), cotton (Ludueña, Vázquez, & Alvarez, 2012), spruce bark (Le Normand, Moriana, & Ek, 2014), sisal fibres (Santos, Rodrigues, Ramires, Ruvolo-Filho, & Frollini, 2015), pineapple leaf fibres (Shih et al., 2014), garlic skin (Reddy & Rhim, 2014), soy hull (Flauzino Neto, Silvério, Dantas, & Pasquini, 2013), rice straw (Boonterm et al., 2015; Kargarzadeh, Johar, & Ahmad, 2017), coconut husk fibres (Rosa et al., 2010), mango seeds (Henrique, Silvério, Neto, & Pasquini, 2013), red algae waste (El Achaby, Kassab, Aboulkas, Gaillard, & Barakat, 2018) or banana peel waste (Hossain, Ibrahim, & AlEissa, 2016) have been evaluated, although no previous studies into the extraction and characterization of cellulosic materials from coffee husk have been reported. However, coffee husks, obtained after de-hulling the coffee cherries during dry processing, also constitute a source of lignocellulosic materials, containing ~57% of cellulosic and ~22% lignin components (Moreno-Contreras, Serrano-Rico, & Palacios-Restrepo, 2009). Likewise, the coffee (*Coffea sp.*) crop generates a significant amount of waste, which could be used as a source of different valuable products (Alves, Rodrigues, Nunes, Vinha, & Oliveira, 2017), with a positive impact on the economy of producing countries, such as Brazil, Vietnam, Indonesia, Colombia, Ethiopia, India or Mexico (Oliveira & Franca, 2015).

On the other hand, rice husk, with a similar composition in lignocellulosic compounds to coffee husk (~55% cellulose and ~35% lignin, Brinchi, Cotana, Fortunati, & Kenny, 2013), has been previously studied as a source of these materials. The previously described methods to obtain and characterize cellulose fibres from rice husk (Johar, Ahmad, & Dufresne, 2012; Kargarzadeh et al., 2017) could be applied to evaluate the

coffee husk's potential as a source of cellulosic fractions, useful as filling compounds in composite materials.

Natural cellulose obtained from these kinds of biomasses can be transformed into micro- and nano-scale materials, yielding products, such as microcrystalline cellulose, microfibrillar cellulose or cellulose nanocrystals (CNC) (Azeredo, Rosa, & Mattoso, 2017; Brinchi et al., 2013; Sanjay et al., 2018) with very good properties as reinforces, at the same time that the this allows for a better exploitation of lignocellulosic residues. The isolated cellulose fibres submitted to different treatments yield different crystalline fractions such as CNCs. These are a good option as reinforcing agent due to their abundant hydroxyl groups, which allows for obtaining different derivative materials with adequate compatibility, high degree of crystallinity, excellent mechanical properties, large specific surface area, high aspect ratio, and high thermal stability (Azeredo et al., 2017; Ng et al., 2015). The final yield of the isolation process depends on the type of initial raw material and process conditions.

The aim of this study was to isolate and characterise the cellulose fibres and cellulose nanocrystals from coffee husks, in parallel with rice husk, for comparison purposes. Likewise, the reinforcing capacity of the isolated cellulose fibres and CNCs, from both coffee and rice husk, have been analysed in corn starch films through their effect on tensile behaviour of the films.

2. Materials and methods

2.1. Materials

Rice husk was obtained from Dacsa (Almàssera, Valencia, Spain) and coffee husk was provided by Centro Surcolombiano de Investigaciones en Café de la Universidad Surcolombiana (Neiva, Colombia). Corn starch was purchased from Roquette (Roquette

Laisa, Benifaió, Spain). Glycerol and sodium hydroxide was purchased from Panreac Química, S.A (Castellar del Vallès, Barcelona, Spain). Sodium chlorite and acetate buffer for bleaching treatment and sulphuric acid (purity 98%) used for acid hydrolysis were provided by Sigma Aldrich Química S.L (Madrid, Spain). For sample conditioning, phosphorus pentoxide (P_2O_5) and magnesium nitrate-6-hydrate ($Mg(NO_3)_2$) were supplied by Panreac Química, S.A. (Castellar del Vallès, Barcelona, Spain). All other chemicals used were reagent grade and underwent no further purification.

2.2. Extraction/purification process applied to rice and coffee husks

The same process conditions for both raw materials were applied, adapted from Johar et al. (2012). Ground rice or coffee husks, with a mean particle size of 2-3 mm, were alkali treated and afterwards submitted to bleaching treatment and acid hydrolysis.

2.2.1. Alkali treatment

Alkali treatment was carried out with a 4 wt% NaOH solution, with a solid solution mass ratio of 1:20, at reflux temperature for 3 h, under continuous stirring. Then, the solid was filtered and washed with distilled water several times until the alkali solution was removed. This treatment was repeated twice.

2.2.2. Bleaching treatment

For bleaching treatment, equal parts of acetate buffer solution, sodium chlorite (1.7 wt%) and water were mixed with the alkali treated solid (1:20 mass ratio) and submitted at reflux temperature for 4 h. This process was repeated as many times as necessary (4 in rice samples and 6 in coffee samples) until the samples were completely white. After

that, the samples were filtered and washed with distilled water several times until the solution was removed.

2.2.3. Acid hydrolysis

Cellulose nanocrystals were prepared by acid hydrolysis of the obtained bleached fibres as described Johar et al. (2012) and Cano et al. (2015). Fibre treatment with sulphuric acid, (64 %, wt/wt) at 50 ºC for 40 min, was carried out under continuous stirring, using 7.5 wt% of fibre content. The hydrolysed cellulose sample was washed several times with distilled water by centrifugation at 14.000 rpm for 30 min to concentrate cellulose material and to remove acid excess. The suspension was then dialysed against distilled water until a constant pH was reached and then neutralised with 10 wt % ion resin (Dowex Marathon MR-3) for 24 h. The resin was separated by vacuum filtration through a Whatman 541 filter, and the filtrate CNC suspension was sonicated for 30 min, using a tip sonicator (Vibra-Cell^{TM} VCX 750, Sonics & Materials, Inc., Newton, USA) in an ice bath and kept refrigerated for further analyses.

2.3. Structural characterization of fibres and cellulose nanocrystals (CNC).

2.3.1. Thermal properties

The thermal stability of the different samples was analysed using a Thermogravimetric Analyzer TGA 1 Star^{e} System analyser (Mettler-Toledo, Inc., Switzerland) under nitrogen atmosphere (gas flow: 10 mL min^{-1}). Samples (about 8 mg) were heated from 25 to 900 ºC at 10 ºC/min (Johar et al., 2012). At least two replicates for each sample were obtained. Initial degradation temperature (Onset) and peak temperature (Peak) were registered from the first derivative of the resulting weight loss curves using the STAR^{e} Evaluation Software (Mettler-Toledo, Inc., Switzerland).

2.3.2. X-ray diffraction

A Diffractometer (XRD, Bruker AXS/D8 Advance) was used to obtain X-Ray diffraction patterns of the different samples conditioned at 25 °C and 53% RH, between 2θ: 5° and 40° using Kα Cu radiation (λ: 1.542 Å), 40 kV and 40 mA with a step size of 0.05°. For this analysis, the samples were milled and spread until covering the sample holder. The degree of crystallinity (X_c) of the samples was estimated from the ratio of crystalline peak areas and the integrated area of XRD diffractograms, using OriginPro 8.5 software, assuming Gaussian profiles for crystalline and amorphous peaks, as described by Ortega-Toro et al. (2016a).

2.3.3. Optical microscopy

Light microscopy (Optika Microscopes B-350 connected to an Optikam B2 camera, Italy) was used to measure the length range of the fibres after alkali and bleaching treatments. A drop (30 μlL of the 1% solid dispersions was spread over the porta and observed at 10X magnification level. The bleached fibres were stained with gentian violet to obtain the adequate contrast.

2.3.4. Scanning Electron Microscopy (SEM)

A Scanning Electron Microscope (JEOL JSM-5410, Japan) was used to analyse the microstructure of the material after different treatments: untreated (C), alkali treated (At) and bleached (Bt) fibres. The fibres were maintained in desiccators with P_2O_5 for 2 weeks at 25 °C and the SEM observations were carried out in duplicate for each material. Samples were gold coated and observed, using an accelerating voltage of 15 kV.

2.3.5. Morphological analysis in CNCs

The particle size distribution of rice and coffee cellulose nanocrystals was analysed by using 2 mL of CNC suspensions in Zetasizer equipment (Zetasizer Nano ZS, Malvern Instruments, U.K). Five measurements were taken for each sample.

Transmission Electron Microscopy (JEOL JEM-1010, Japan) was also used to analyse morphology and the size of the CNCs. A drop of diluted CNC dispersion was deposited on the carbon film supported by the copper grid. TEM analysis was performed at an accelerating voltage of 80 kV. The aspect ratio (Ar) (L/*d*, L mean length and *d* mean diameter) was measured in 100 individualised crystals of each sample, from the digital images recorded with an AMT V600 camera, using the ImageJ software.

2.3.6. Chemical composition

The contents of cellulose, hemicellulose, lignin and ashes of the rice and coffee husk samples submitted to the different treatments were determined according to the NREL standard method for biomass (NREL/TP-510-42618, 2011), applying sulphuric acid hydrolysis to the samples and determining the cellulose and hemicellulose content from the glucose, xylose and arabinose amounts determined by HPLC (Hitachi LaChrom, Japan) in the sample hydrolysate. The Biorad Aminex HPX-87H column and an IR detector (Agilent 1200 series RID) were used. The injection volume of all samples was 60 µL, and 5 mM sulphuric acid has been used as mobile phase at 0.5 mL/min flow rate and 65 °C. Data acquisition was carried out by using Galaxie Chromatography Data System. Raw husk powders were first water extracted, according to the method recommendation (NREL/TP-510-42619, 2008) to avoid interferences in the HPLC analysis. Lignin and ashes were also determined from the acid insoluble fraction by

filtration, desiccation and incineration. Total ashes were analysed in the whole sample by sample incineration at 575 ºC for 24 h.

2.3.7. Reinforcing capacity of the cellulose fibres and CNCs

The reinforcing capacity of 1 wt % of cellulose fibres and CNCs was evaluated in corn starch films containing 30 % glycerol, obtained by melt blending (using Model LRM-M-100, Labtech Engineering, Thailand roller) and compression moulding (using Model LP20, Labtech Engineering, Thailand press). Pellets of thermoplastic starch (with or without filler) were obtained at 160 ºC in the roller-mill using a prepared dispersion of the starch-glycerol-filler-water (1:0.3:0.01:0.5). The pellets conditioned at 53% relative humidity (RH) were compressed at 130 bars and 160ºC for 8 min, and cooled down to 50ºC for 3 min.

The obtained films were conditioned at 53% RH and 25 ºC for 1 week and analysed as to the tensile behaviour (ASTM standard method D882; ASTM, 2001), using a universal test machine (TA.XTplus model, Stable Micro Systems, Haslemere, England). Rectangular film samples (2.5 x 10 cm) were submitted to the tensile test at 50 mm/min till break. Tensile strength-Henky strain curves were obtained and elastic modulus, tensile strength and deformation at break were determined for each sample. Ten replicates were carried out for each film sample.

2.3.8. Statistical analysis

Statgraphics Plus for Windows 5.1 (Manugistics Corp., Rockville, MD) was used for statistical analyses of data through analysis of variance (ANOVA). Fisher's least significant difference (LSD) was used at the 95% confidence level.

3. Results and discussion

3.1. Morphological changes and yield in alkali and bleaching treatments of rice and coffee husk.

The effect of the different treatments on the appearance of the raw material can be observed in Fig. 1a, 1b and 1c. Alkali treatment provoked a colour change in both rice and coffee husk samples, the former turning more brownish whereas the latter became brownish-orange, which could be associated with the different pigmentation of the lignin fraction remaining in the material. This treatment was effective at purifying the cellulose fibres, removing non-cellulosic components, such as a part of the lignin fraction, hemicellulose, pectin and wax (Kallel et al., 2016). After the bleaching treatment, the sample colour change was more evident and the samples exhibited the characteristic whiteness of cellulose fibres, where extensive extraction of cementing compounds, such as lignin, occurred. Table 1 shows the sample composition of the products submitted to the different treatments, where the contents in lignin, hemicellulose, cellulose and ashes are shown. The progressive enrichment in cellulose of the husk products can be observed after the successive treatments. Cellulosic fibres obtained after bleaching still contained a fraction of hemicellulose in both rice and coffee products and the cellulose enrichment of the rice sample was slightly lower than the 96% reported by Johar et al. (2012), applying similar treatments to rice husks.

The cellulose and lignin content of the husk samples ranged between 34-35% and 22-23 %, respectively, showing lower values than those previously reported by other authors. Brinchi et al. (2013) reported about 55% and 36% for cellulose and lignin content in rice husk, respectively, while Moreno-Contreras et al. (2009) quantified about 57% cellulose and 22% lignin in coffee husk. Both coffee and rice husks contained a similar

amount of cellulosic compounds, which agrees with the similar solid yield obtained for both products after the alkali and bleaching processes.

Table 1. Chemical composition (wt. percentage) of the rice (R) and Coffee (C) husk samples at the different treatment step (untreated: C, alkali treated: At, bleaching treated: Bt)

Samples	Water extractables (%)	Cellulose (%)	Hemicellulose (%)	Lignin (%)	Ashes (%)
R-C	14.5 ± 0.9	33.8 ± 0.5	17.1 ± 0.2	21.5 ± 0.3	16.5 ± 0.4
R-At	-	55.9 ± 0.3	15.8 ± 0.4	19.9 ± 0.8	0.59 ± 0.05
R-Bt	-	73.8 ± 0.3	19.2 ± 0.7	1.6 ± 0.5	0.14 ± 0.03
C-C	17.8 ±1.4	35.4 ± 0.9	18.2 ± 1.3	23.2 ± 0.5	1.4 ± 0.3
C-At	-	52.6 ± 1.1	19.0 ± 0.2	20.4 ± 0.6	0.74 ± 0.15
C-Bt	-	61.8 ± 2.6	27.2 ± 0.9	2.6 ± 0.4	0.49 ± 0.19

Alkali treatment yielded 86 and 88 % with respect to the initial dry powder of rice and coffee husks, respectively, while this yield was 48 and 60 %, respectively, for the bleaching treatment, which produced a cellulose-rich sample (41 and 53 %, respectively with respect to the initial mass). Moreover, taking the final cellulose content of each bleached product into account, a better purification of the rice husk cellulosic fraction than that of the coffee husk was reached. The cellulose content found in different lignocellulosic wastes varies between 40-80 %. Jonoobi, Ahmad & Dufresne (2015) reported cellulose and lignin contents of different raw materials, such as kenaf stem (~58%, ~17.5%), wheat straw (~43%, ~22%), pineapple leaf (~81%, ~3.5%) and banana rachis (~48%, ~12%).

After treatments, the particle size of the ground raw materials (2-3 mm) was drastically reduced, as reflected in the light microscopy images (Fig. 1c and 1e), in which the fibre length ranges are shown after the alkali and bleaching treatments. Particle size reduction

provoked by bleaching treatment was similar for both husk materials and reflects the effective attack of the chemical agents disrupting the internal structure of the material while removing the non-cellulosic components. Other authors reported different fibre sizes depending on the raw material. As examples, bleached water hyacinth fibre was 25–50 µm in size (Sundari & Ramesh, 2012); bleached garlic straw filaments were about 14-17 µm length (Kallel et al., 2016) and pineapple leaf fibres were in the range of 50-12 µm (Cherian et al., 2011). The main difference between cellulosic rice and coffee fibres are the trend to aggregate in the water dispersion. Whereas coffee fibres appear as scattered elements, rice fibres are flocculated in the aqueous medium (Fig. 1, R-Atc). This suggests the action of more attractive forces between particles despite the similarity in size and composition, which could be associated to different surface bonded molecules.

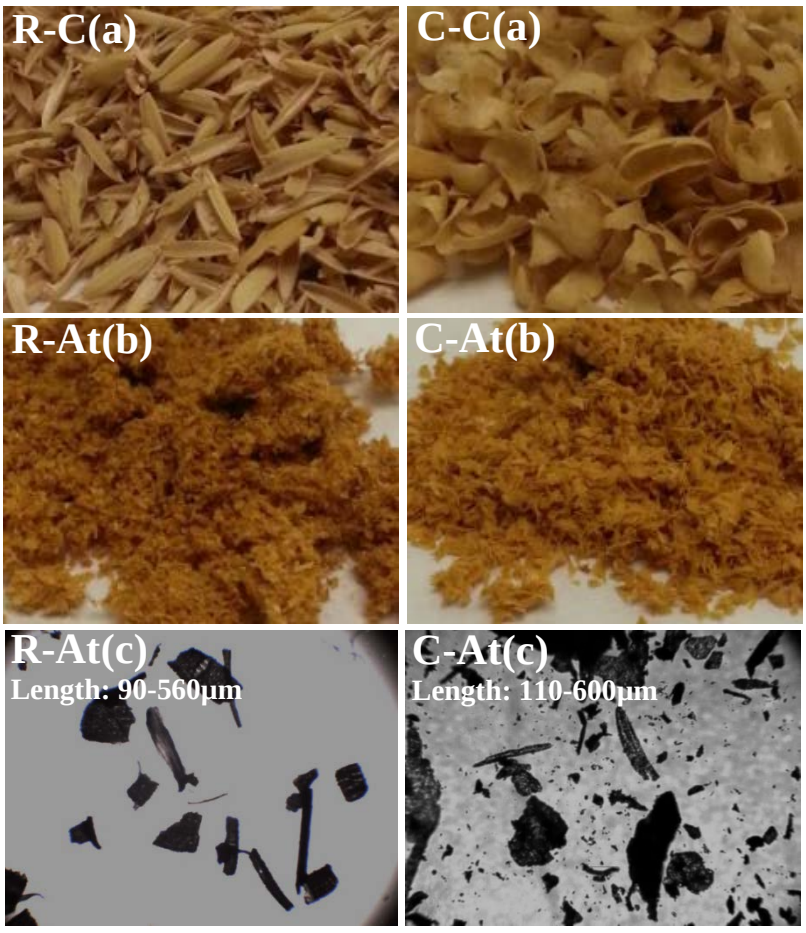

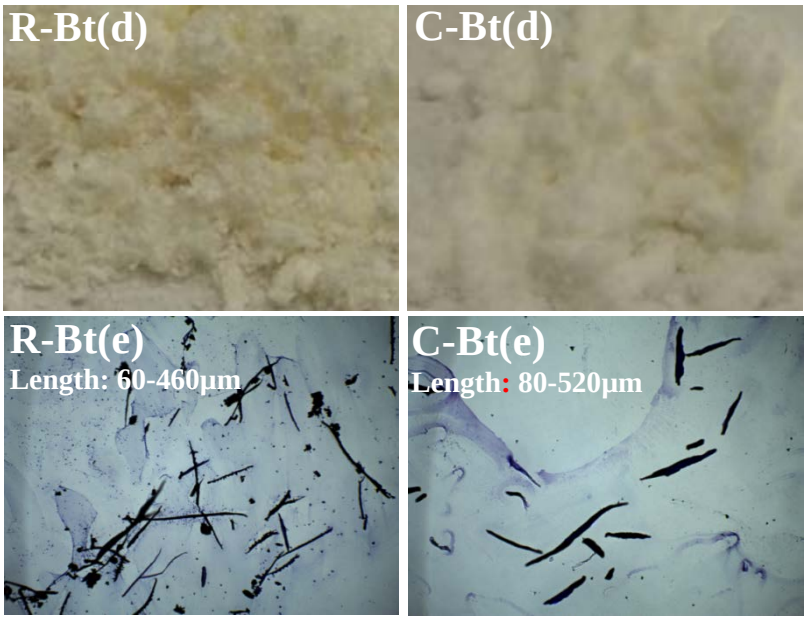

Fig. 1. Appearance of rice (R) and coffee (C) husk samples after each treatment: untreated sample (control: C-a), alkali treatment (At-b), bleaching treatment (Bt-d). Light micrographs of rice and coffee husk fibres after alkali (At-c) and bleaching treatment (Bt-e).

3.2. Micro- and Nano-structural analysis

Fig. 2 shows SEM micrographs of the rice and coffee fibres, either untreated or submitted to the different treatments, where the structural changes produced by the successive processes can be observed. In the raw material, an ordered and homogeneous organisation could be distinguished evidencing the natural arrangement of the constituents. In both samples, the fibres are arranged in parallel and an ordered assembly can be observed, while pectin and intercellular junctional material fill the cell unions. Wax crystals covering the sample surface can also be seen, mainly in rice husk, which showed a rougher appearance. After the alkali treatment, the fibre surface becomes rougher due to the losses in the outer non-cellulosic compounds (hemicellulose, lignin, pectin and wax). This change was more appreciable in rice husk.

Both wax and pectin are known to surround the surface of natural fibres as a protective layer. In both cases, fibre bundles remain after alkali treatment, which indicates the retention of the cementing lignin material, which acts as a binder in the fibre components and preserves the bundle shape during the alkali treatment. Nevertheless, a great part of the pectin and hemicellulose content was removed from the fibres during this treatment, according to previous studies (Batra, 1981; Johar et al., 2012). The appearance of coffee husk samples reveals a less aggressive effect of the alkali treatment, which can be explained by its different composition. In fact, the product yield in the alkali treatment was higher in coffee than in rice husk, which could be due to a lower extraction of components in this product, as reflected in sample composition (Table 1).

The alkali process is more effective when the biomass has low lignin content and the process yield depends on the raw material and treatment conditions. Treatment with sodium hydroxide decreases the degree of polymerization and crystallinity in the material, disrupts the lignin structure and increases the internal surface of cellulose fibres (Singh, Shukla, Tiwari, & Srivastava, 2014). All of this favours the penetration of the bleaching agents into the structure (Kallel et al., 2016).

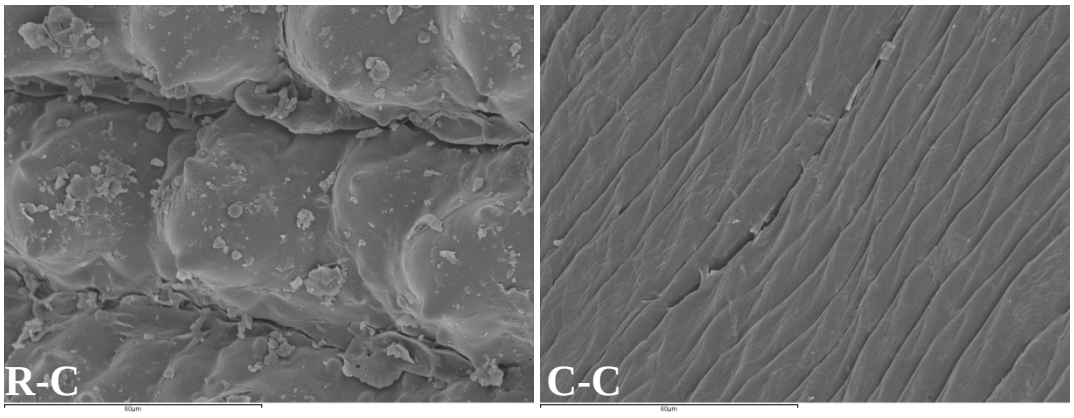

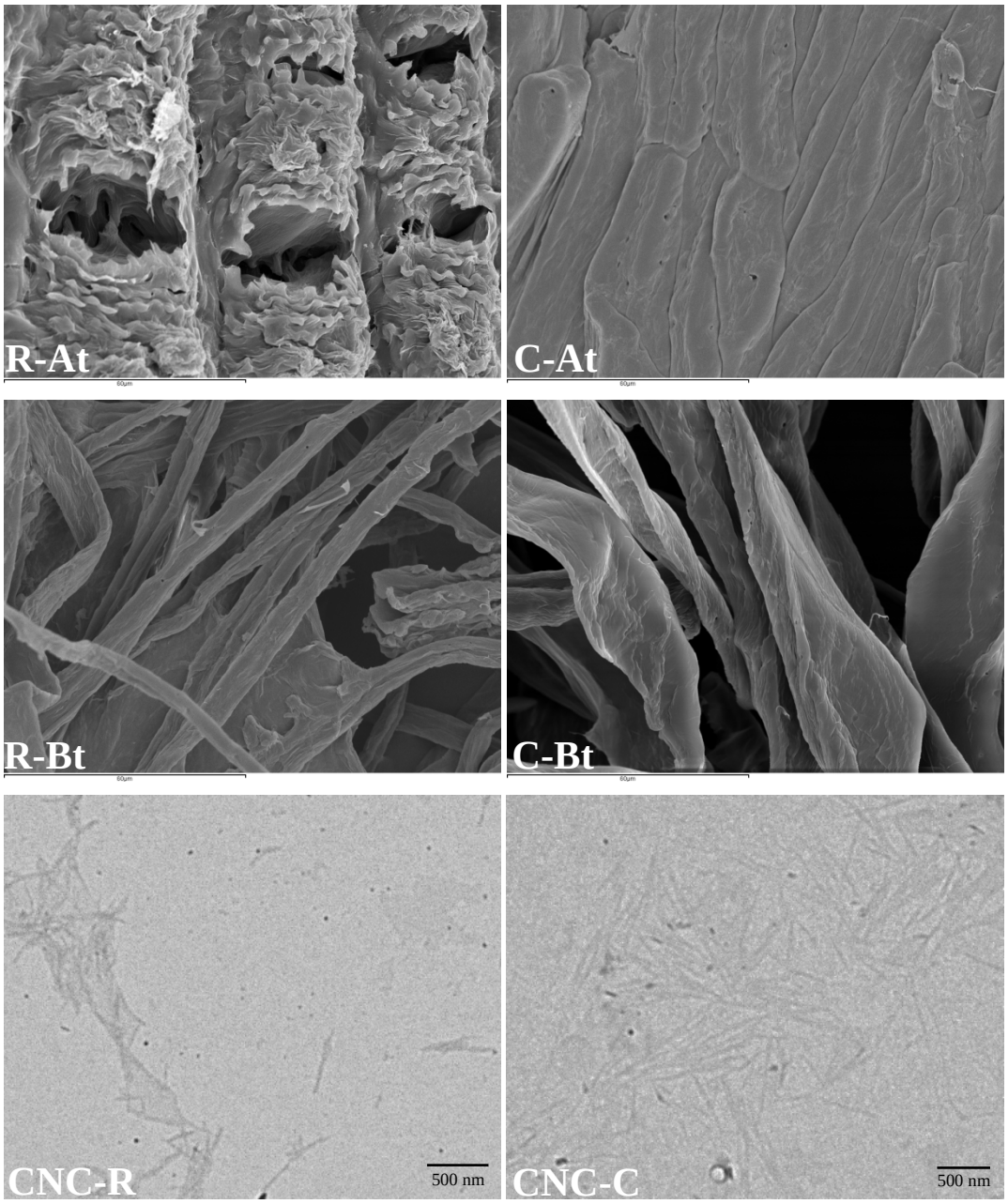

Fig. 2. SEM micrographs of the rice and coffee husks untreated (R-C or C-C) and after the alkali (R-At or C-At) and bleaching treatments (R-Bt or C-Bt). TEM micrographs of nanocrystals obtained from rice (CNC-R) and coffee (CNC-C) bleached fibres are also shown.

In both husk materials, the subsequent bleaching treatment was very effective at separating isolated fibres, as observed in Fig. 2 (R-Bt and C-Bt). The rice and coffee husk fibre bundles separate into very thin individual fibres with different diameters, thus

indicating the great efficacy of the treatment to eliminate the non-cellulosic components, as previously reported (Chen et al., 2011; Espino et al., 2014; Savadekar & Mhaske, 2012). In the treatment, sodium chlorite becomes chlorine dioxide in acetate buffer solution, provoking the oxidation of the lignin aromatic ring (Ng et al., 2015; Ni, Kubes, & Van Helnlngen, 1993; Zainuddin, Ahmad, Kargarzadeh, Abdullah, & Dufresne, 2013). Coffee fibres were flatter and mainly helically folded, while rice fibres were similar to those previously reported by Johar et al. (2012), more cylindrical of less than 10 μm in diameter. The fibres diameters were in the range of previously reported for other plant wastes such as bleached garlic straw (Kallel et al., 2016). The obtained cellulose fibres showed a very high aspect ratio (L/d, L being the length and d the diameter), which provides them with adequate properties as reinforcing materials for composite applications.

The Van der Waals forces and hydrogen bonds that act in the crystalline zones of the cellulose provide high resistance to acid attack, while the amorphous regions are disordered and prone to sulfuric acid hydrolysis (Khalil et al., 2016; Qiao, Chen, Zhang, & Yao, 2016). Thus, the sulphuric acid treatment removes the cellulose fibres of the amorphous zones and reduces the fibre size to nanometric scale (Azizi Samir, Alloin, & Dufresne, 2005). Therefore, observations of the isolated CNCs were carried out by TEM at higher magnification. Fig. 2 also shows micrographs of the CNCs with a short, rod-like structure and many aggregates. These aggregates emerged in the drying step for sample preparation due to strong intermolecular hydrogen bonds between the particles (Sung et al., 2017). Likewise, the particle morphology and aggregation is highly affected by the TEM sample preparation (Chauve, Fraschini, & Jean, 2013; Kaushik, Fraschini, Chauve, Putaux, & Moores, 2015). However, some specimens remained isolated, which allows for the characterisation of their length and diameter and so, their

361 aspect ratio, from digital images recorded with the camera and the use of the image
362 analysis software. Fig. 3a and 3b show the distribution of diameter and aspect ratio of
363 CNCs extracted from rice and coffee husk fibres. Length (L) and width (d) of rice CNC
364 were 310 ± 160 and 39 ± 13 nm, and similar values were obtained for coffee CNC (310
365 ± 160 and 20 ± 4 nm, respectively), the latter being slightly thinner. Most of the CNCs
366 exhibited an aspect ratio (L/d) in the range of 10-20 for both husk materials. These were
367 similar both to those obtained by Johar et al. (2012) for rice husk and to the values
368 reported for different lignocellulosic materials, such as ramie fibres (Habibi &
369 Dufresne, 2008), bagasse pulp (Bras et al., 2010), sugarcane bagasse (Hassan M.L,
370 Mathew, Hassan E. A, El-Wakil, & Oksman, 2012), kenaf fibres (Kargarzadeh et al.,
371 2012), banana peel (Khawas & Deka, 2016) or *Alfa tenassissima* (BenMabrouk, Wim,
372 Dufresne, & Boufi, 2009). Kallel et al. (2016) report that the aspect ratio of CNC
373 extracted from different materials usually vary from 10 to 70, although the highest
374 values (L/d = 80) were obtained in CNC extracted from garlic straw (Kallel et al., 2016)
375 and tunicate (*Polycarpa aurata*), a sea animal with external cellulosic microfibrils, (L/d
376 = 50-200) (Anglès & Dufresne, 2000). Silvério et al. (2013) reported that CNC could be
377 considered as a good reinforcing material if their aspect ratio exceeds a value of 10. The
378 CNCs dimensions ranges from 2 to 20 nm in diameter and from 100 to 600 nm in length
379 (Moriana, Vilaplana, & Ek, 2016), depending on the nature of the lignocellulosic raw
380 material, purification, mechanical process, pre-treatment and conditions of acid
381 hydrolysis (Chauve et al., 2013).
382 Fig. 3c also shows the hydrodynamic diameter distribution of the isolated CNCs for
383 water suspensions of CNC from rice and coffee husks obtained from dynamic light
384 scattering analysis. Hydrodynamic diameter corresponds to that of an equivalent
385 spherical specimen that would have the same diffusion coefficient and, for rod-like

386 particles, such as CNCs, are only used for qualitative comparisons. The obtained
387 hydrodynamic diameter distributions were similar to that reported by Kallel et al. (2016)
388 for CNCs obtained from garlic straw. The z-average values and peak values for each
389 sample are also shown in Fig. 3c. This average size, related with the hydrodynamic
390 volume of the crystals, and the wide distribution reflects the aggregation tendency of
391 CNC in the aqueous media. CNC from coffee husk were smaller and with lower
392 tendency to aggregate as revealed by the smaller z-average and narrow distribution.
393 This agrees with the behaviour deduced from the microscopic observations.
394 Given the crystalline nature of cellulose, contrary to the amorphous nature of
395 hemicellulose and lignin, the crystallinity of the natural fibres rises as the extraction
396 progresses with the different chemical treatments. Indeed, the alkali treatment increases
397 the stiffness of the fibre as it removes different amorphous fractions.

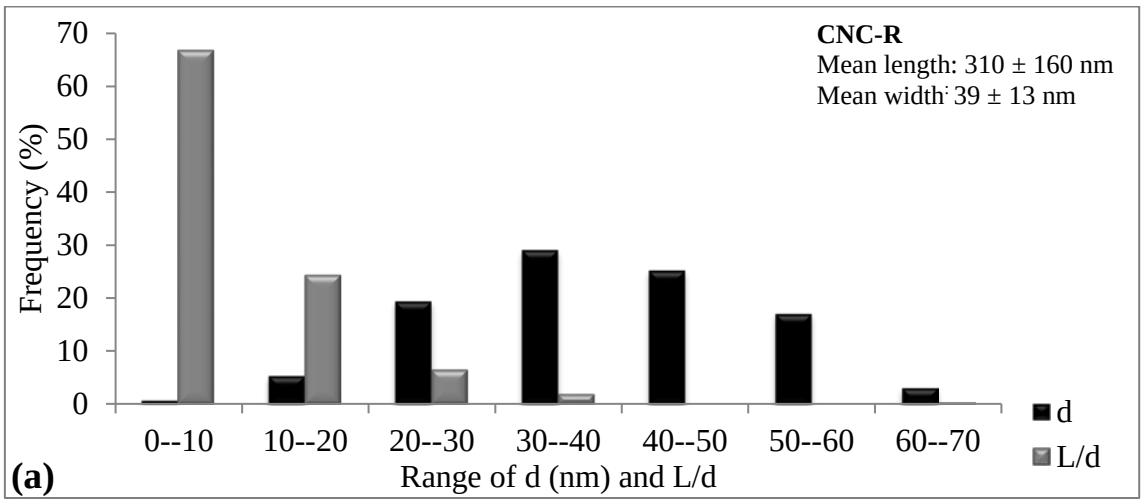

398
399

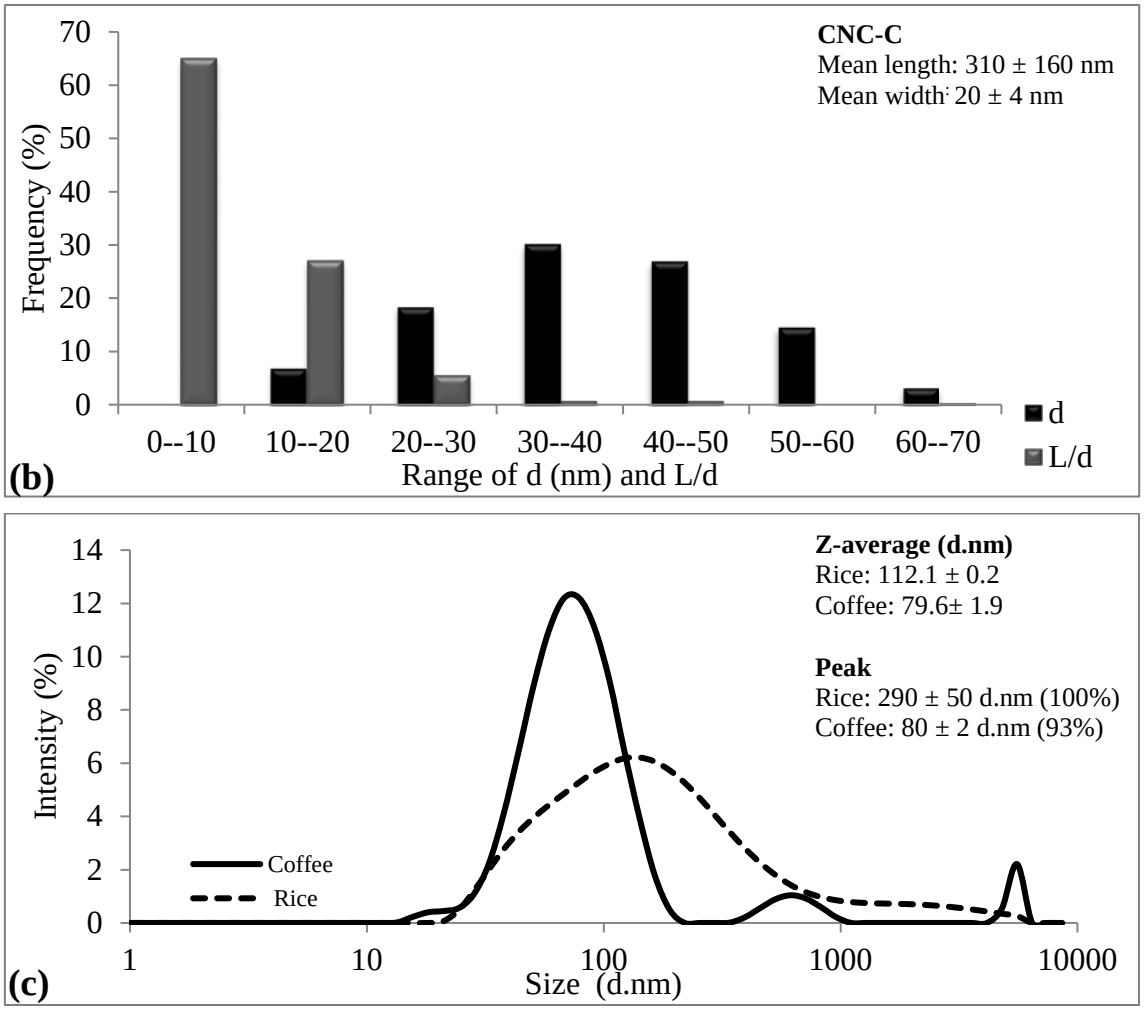

Fig. 3. Diameter distribution and aspect ratio of the CNC extracted from rice (a) and coffee (b) bleached fibres. Particle size distribution from dynamic light scattering of the CNC aqueous dispersion from rice and coffee samples (c).

Acid treatment does not affect the crystalline domains, but destroys the amorphous region of the fibre (Fengel & Wegener, 1984). Then, the X-ray diffraction spectra of the different products obtained after each treatment were analysed to control the progressive enrichment in crystalline cellulose.

Fig. 4 shows the X-ray diffraction patterns of the untreated, alkali treated and bleached fibres as well as of the isolated CNC of rice and coffee fibres. In all samples, the typical crystalline peaks of type I cellulose (2θ: 15-16º [110], 22º [200] and 34º [004]) were observed as reported by other authors (Johar et al., 2012; Kallel et al., 2016; Savadekar

& Mhaske, 2012). As expected, these peaks become more defined upon each chemical treatment. Likewise, the degree of crystallinity (Xc) in the different samples was estimated from the ratio between the area of the peaks and the total area under spectra which include the amorphous response (Ortega-Toro et al., 2016a). The crystallinity degree increased after each chemical treatment, according to the progressive removal of components of the amorphous fraction (Bettaieb et al., 2015; Le Normand et al., 2014; Sheltami, Abdullah, Ahmad, Dufresne, & Kargarzadeh, 2012). This increase was more noticeable in the last acid treatment when the amorphous regions of cellulose were also eliminated and CNC were purified. During the hydrolysis process, hydronium ions can penetrate the more accessible amorphous regions of cellulose provoking the cleavage of glycosidic bonds, releasing individual crystallites (Lima & Borsali, 2004), which can grow or realign in parallel, thus increasing the cellulose crystallinity (Li et al., 2009). CNC exhibited high crystallinity due to the chemical cellulose structure, where each monomer has three hydroxyl groups with the ability to form intra- and inter-molecular hydrogen bonding between cellulose chains giving rise to a highly compact system (Ng et al., 2015; Siqueira, Bras, & Dufresne, 2010). The high degree of crystallinity confers stiffness on the CNC and so a reinforcing capability when included in other polymer materials.

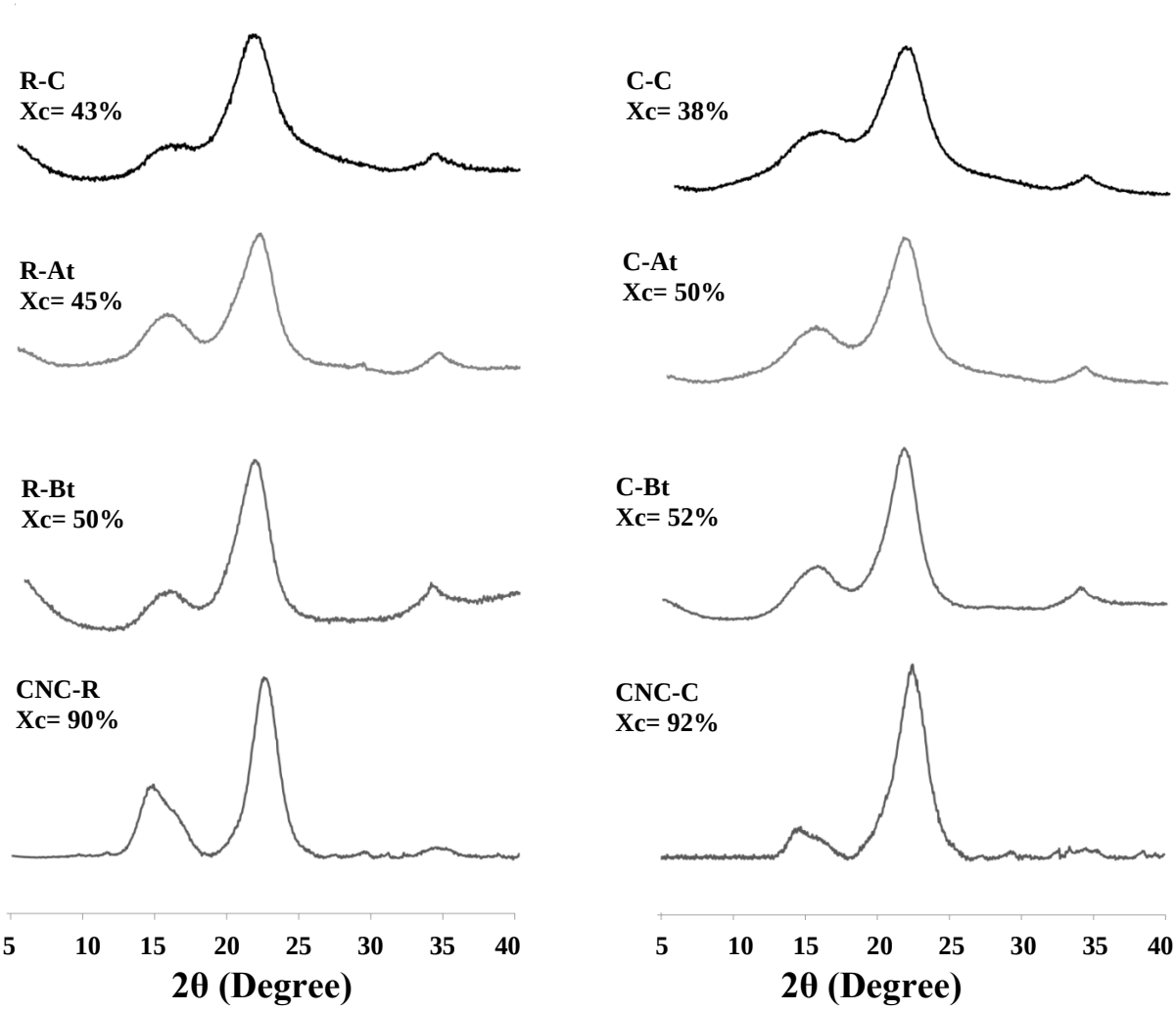

Fig. 4. X-Ray diffraction patterns of rice and coffee husks untreated (C), alkali treated (At), bleaching treated (Bt) and acid hydrolysed (CNC).

3.3. Thermal analysis

Thermogravimetric analysis allows us to obtain information about how the thermal stability of the material changes in line with the different treatments. The progressive extraction of low molecular weight compounds leads to the enhancement of the thermal stability.

Fig. 5 shows the TGA and DTG curves of the rice and coffee husk samples, untreated and submitted to the different treatments. The peaks associated with the different weight losses caused by thermal degradation can be observed in DGTA curves. All samples

exhibit a small weight loss below 100ºC, which can be attributed to the elimination of physically adsorbed water in the samples. The other peaks are associated with the thermal degradation of the lignocellulosic compounds. Table 2 summarises thermal degradation temperatures (onset and peak) for both rice and coffee samples submitted to the different chemical treatments. The first degradation step in untreated samples, around 271-279 ºC, can be attributed to the decomposition of hemicelluloses and a part of the lignin fraction (Shebani, Van Reenen, & Maincken, 2008) and was very similar in both husk samples. In all samples, the peak around 300 ºC is attributable to cellulose and lignin decomposition. Mensaray & Ghaly (1998) reported that lignocellulosic materials decompose in the temperature range of 150-500 ºC. Specifically, hemicellulose decomposes mainly from 150 to 350 ºC, cellulose at between 275 and 350 ºC and lignin undergoes gradual decomposition in the range of 250-500 ºC. As shown in Table 2, the rice and coffee samples exhibited similar thermal behaviour, similarly affected by chemical treatments.

Two decomposition peaks were observed in both untreated material associated to the successive degradation of the different lignocellulosic fractions. However, only one peak appeared after after alkali treatment in both cases, which can be attributed to the loosening of the low molecular weight lignin fragments, which degrade at lower temperatures (Johar et al., 2012). After the bleaching treatment, a significant increase in degradation temperature was observed due to the removal of hemicellulose and lignin fractions and the higher content of cellulose.

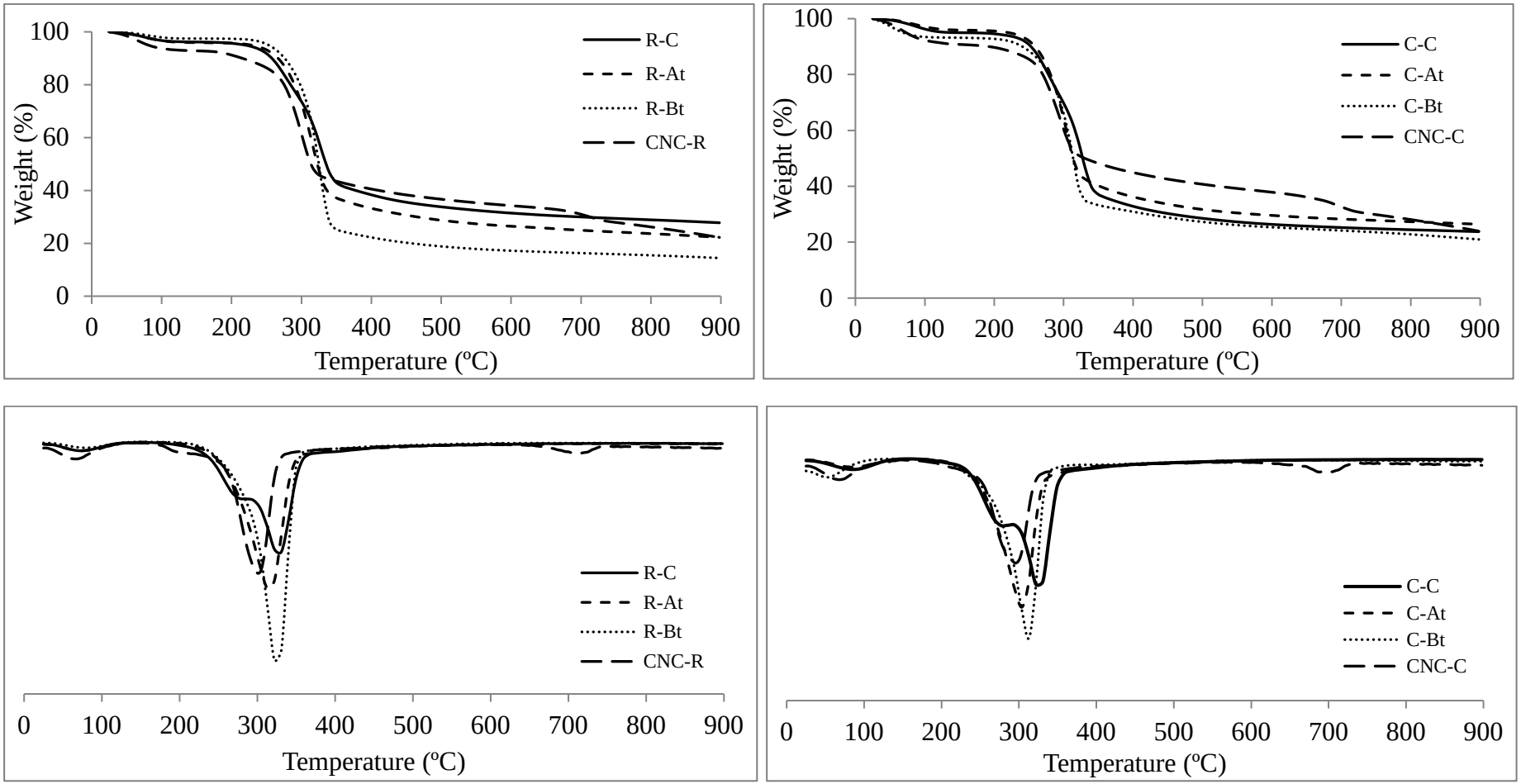

Fig. 5. TGA and DTG curves of rice and coffee husks untreated (C), alkali treated (At), bleaching treated (Bt) and acid hydrolysed (CNC).

The residual mass at temperature around 400–700 ºC in raw rice husks fibre were remarkably high (more than 30%), which is due to the high content of ash and lignin (Fahma, Iwamoto, Hori, Iwata, & Takemura, 2011) as well as to the high silica content of the rice husk, all of these contributing to the high char content for raw fibres. Similar thermogram patterns have also been reported on raw rice husk fibres (Johar et al., 2012). For coffee husk no remarkable differences on the mass resides were observed for untreated and treated fibres, all these being lower than 30%, according to the lower ash content of the material. The isolated, more crystalline cellulose fraction from the acid treatment had a lower degradation temperature in both husk products, which has been attributed to the surface sulphation resulting from the sulphuric acid treatment (Johar et al., 2012) by the replacement of hydroxyl groups of the cellulose structure by sulphate groups throughout the hydrolysis process (Jonoobi et al., 2015; Siqueira et al., 2010). Moreover, this treatment induces an increase in the char fraction compared to the bleached fibres, also due to the introduction of sulphated groups which act as flame retardants (Roman & Winter, 2004). However, at about 700 ºC, a final mass loss step was observed in both acid hydrolysates, reflecting the action of a final degradation mechanism, which led to a similar residual mass to the bleached fibres and which was not observed in previous studies on rice husk cellulosic materials (Johar et al., 2012).

The small differences in the thermal behaviour of rice and coffee husk can be explained by the compositional differences, since thermal degradation of cellulose-based fibres is significantly influenced by their structure and composition.

Table 2. Mean values and standard deviation of onset and peak temperatures for thermal degradation of rice and coffee husks of each stage of treatment (untreated: C, alkali treated: At, bleaching treated: Bt).

	[245-280]ºC		[248-330]ºC	
Samples	**Onset (ºC)**	**Peak (ºC)**	**Onset (ºC)**	**Peak (ºC)**
R-C	247.6 ± 0.5^{b}	271.1 ± 0.7^{a}	301.8 ± 0.2^{f}	329.8 ± 0.7^{f}
R-At	-	-	263 ± 4^{c}	317.3 ± 1.4^{d}
R-Bt	-	-	292.4 ± 0.6^{e}	326.8 ± 0.2^{e}
CNC-R			261.8 ± 0.4^{c}	301.2 ± 0.3^{b}
C-C	245.0 ± 0.4^{a}	279.16 ± 1.12^{b}	302.6 ± 1.2^{f}	327.8 ± 0.7^{ef}
C-At	-	-	254.1 ± 0.4^{b}	304.8 ± 1.2^{c}
C-Bt	-	-	280 ± 3^{d}	315.6 ± 2^{d}
CNC-C			248.9 ± 0.4^{a}	295.6 ± 1.1^{a}

Different superscript letters within the same column indicate significant differences among formulations ($p < 0.05$).

3.4. Reinforcing capacity of the cellulose fibres and CNCs

Starch is one of the most widely studied thermoplastic biopolymers because it is an abundant material, cheap, renewable and biodegradable (Ortega-Toro, Collazo-Bigliardi, Talens, & Chiralt, 2016b). Thermoplastic starch (TPS) film matrices exhibit high barrier properties to oxygen, carbon dioxide and lipids (Ghanbarzadeh, Almasi, & Entezami, 2011), although they have limited mechanical properties and are highly water sensitive. Different studies revealed the improvement in mechanical properties of starch films by the incorporation of cellulosic materials, especially CNCs from different sources (Kargarzadeh et al. 2017; Zainuddin et al, 2013). Likewise, CNCs also increased the film hydrophobicity, reducing the water vapour permeability (Slavutsky & Bertuzzi, 2014) and water uptake capacity (Kargarzadeh et al., 2017). In this sense, cellulosic materials (isolated fibres and CNCs) obtained from rice or coffee husks were incorporated into TPS films in order to analyse their reinforcing ability in this biopolymer matrix.

Fig. 6 shows the tensile behaviour of corn starch films containing, or not, cellulosic reinforcing agents, where the values of the elastic modulus (EM), tensile strength (TS)

518 and percentage deformation (E) at break are also shown. Both cellulosic fibres and
519 CNCs enhanced the elastic modulus of the films, reflecting the reinforcing capacity of
520 both cellulosic fractions. Nanocrystals provoked a higher increase in the film elastic
521 modulus than fibres, while rice husk crystals were more effective at reinforcing the TPS
522 network (186 and 121% higher elastic modulus, respectively for rice and coffee husk
523 CNCs). However, no significant differences were observed for the effect of cellulosic
524 fibres, which increased the elastic modulus of TPS films by 60 %. Other authors also
525 observed better reinforcing properties for nanocrystals than for fibres, by incorporating
526 multiscale kenaf fibres (Zainuddin et al., 2013) or rice husk (Kargarzadeh et al. 2017)
527 fibres in cassava starch films, due to the higher surface area and aspect ratio of the
528 nanocrystals. As previously reported, the mechanical impact of CNCs on TPS films can
529 be, in part, explained by the formation of a percolating network within the polymer
530 matrix, where the stress is assumed to be transferred through crystal-crystal interactions
531 and crystal-polymer matrix interactions (Fortunati et al., 2013). According to the
532 statistical percolation theory for cylindrically shaped particles (Favier, Cavaille,
533 Canova, & Shrivastavas, 1997), the critical percolation volume fraction (percolation
534 threshold: X_P) can be estimated from the particle aspect ratio (Ar) as 0.7/Ar. For the
535 composite films with CNCs, X_P could be estimated as 0.09 and 0.045, respectively for
536 rice and coffee crystals, considering the respective Ar values (7.9 and 15.6). So, the
537 percolation threshold was reached in the nanocomposites and percolation network
538 formation can explain the enhancement of the mechanical behaviour of the films
539 containing CNCs.
540 As concerns resistance and elongation at break, all cellulosic materials provoked a
541 decrease in the film extensibility, except coffee husk fibres which did not significantly
542 affect the stretchability and resistance of the TPS films. Reduction of the elongation

capacity at break implied slightly lower values of the corresponding resistance. Other authors also observed the reinforcing effect of starch films by CNCs, through the enhancement of the elastic modulus, although the film stretchability became more limited (González K, Retegi, González A, Eceiza, & Gabilondo, 2015). This was attributed to the stronger affinity between glycerol and the nanocrystal phase, as deduced from the dynamic mechanical analyses (DMA), which show an increase in the relaxation temperature of the material with the addition of nanocrystals (González et al. 2015).

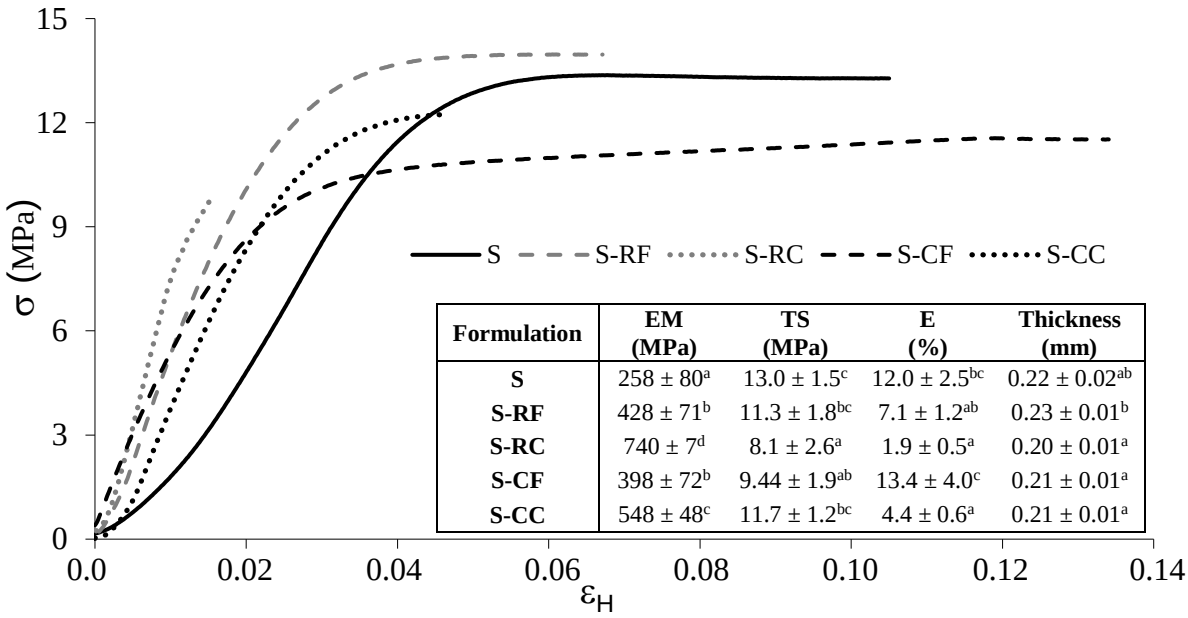

Formulation	EM (MPa)	TS (MPa)	E (%)	Thickness (mm)
S	258 ± 80^{a}	13.0 ± 1.5^{c}	12.0 ± 2.5^{bc}	0.22 ± 0.02^{ab}
S-RF	428 ± 71^{b}	11.3 ± 1.8^{bc}	7.1 ± 1.2^{ab}	0.23 ± 0.01^{b}
S-RC	740 ± 7^{d}	8.1 ± 2.6^{a}	1.9 ± 0.5^{a}	0.20 ± 0.01^{a}
S-CF	398 ± 72^{b}	9.44 ± 1.9^{ab}	13.4 ± 4.0^{c}	0.21 ± 0.01^{a}
S-CC	548 ± 48^{c}	11.7 ± 1.2^{bc}	4.4 ± 0.6^{a}	0.21 ± 0.01^{a}

Fig. 6. Tensile behaviour of corn starch films without (S) and with 1wt% cellulose fillers (S-CF: with coffee husk fibres, S-RF: with rice husk fibres) and CNCs (S-CC: with CNCs from coffee husk, S-RC: with CNCs from rice husk).

4. Conclusions

The cellulose contents of rice and coffee husks were similar in the range of 34-35 %, which make them a good source of cellulosic material for different industrial uses. Purification of cellulose, using the classical alkali and bleaching treatments was

effective at removing hemicellulose and lignin, providing white fibres with about 50% crystallinity degree and 60-500 μm length, with good thermal stability (thermo-degradation T peak: 315-327ºC). Coffee fibres were flatter and more helically folded than rice fibres. Acid hydrolysis of both fibres gave rise to CNCs, with small morphological differences. CNCs from coffee husk were slightly thinner (20 against 39 nm, in average diameter), but with similar aspect ratio (higher than 10). The CNCs exhibited slightly lower thermal stability than the cellulose fibres (thermo-degradation T peak: 249-362ºC). The properties of cellulosic fractions from rice and coffee husk make them very adequate as reinforcing materials in biopolymer composites, especially nano-sized reinforcement (CNCs from rice and coffee husks) which increased the elastic modulus of TPS films by 186 % and 121 %, respectively. So, coffee husk represents an interesting source of cellulosic reinforcing material, whose use in different applications, such as packaging materials, could boost the value of this waste.

Acknowledgements

The authors thank the Ministerio de Economía y Competitividad (Spain) for the financial support provided through Project AGL2016-76699-R. Authors also thank the Electron Microscopy Service of the UPV for their technical assistance.

References

Alves, R. C., Rodrigues, F., Nunes, M. A., Vinha, A. F., & Oliveira M. B. P. P. (2017). State of the art in coffee processing by-products. In: C. M. Galanakis (Ed.), *Handbook of Coffee Processing By-Products* (pp. 1-26). Cambridge: Academic Press.

592 Anglès, M. N., & Dufresne, A. (2000). Plasticized starch/tunicin whiskers
593 nanocomposites. 1. Structural analysis. *Macromolecules*, 33, 8344-8353.
594 ASTM. (2001). Standard test method for tensile properties of thin plastic sheeting.
595 Standard Designations: D882. *In Annual book of ASTM standards*. Philadelphia,
596 PA: American Society for Testing and Materials.
597 Azeredo, H. M. C., Rosa, M. F., & Mattoso, L. E. C. (2017). Nanocellulose in bio-
598 based food packaging applications. *Industrial Crops and Products*, 97, 664-671.
599 Azizi Samir, M. A. S., Alloin, F., & Dufresne, A. (2005). Review of recent research
600 into cellulosic whiskers, their properties and their applications in nanocomposite
601 field. *Biomacromolecules*, 6, 612-626.
602 Balaji, A.B., Pakalapati, H., Khalid, M., Walvekar, R., & Siddiqui, H. (2017). Natural
603 and synthetic biocompatible and biodegradable polymers. In: N. Gopal Shimpi
604 (Ed.), *Biodegradable and Biocompatible Polymer Composites* (pp. 3-32). United
605 Kingdom: Woodhead Publishing.
606 Bassas-Galia, M., Follonier, S., Pusnik, M., & Zinn, M. (2017). Natural polymers: a
607 source of inspiration. In: G. Perale, & J. Hilborn (Eds.), *Bioresorbable Polymers for*
608 *Biomedical Applications* (pp. 31-64). United Kingdom: Woodhead Publishing.
609 Batra, S.K. (1981). Other long vegetables fibres. In: M. Lewin, E. M. Pearce (Eds.),
610 *Handbook of Fiber Science and Technology*. New York: Marcel Dekker Inc.
611 BenMabrouk, A., Wim, T., Dufresne, A., & Boufi, S. (2009). Preparation of
612 Poly(styrene-*co*-hexylacrylate)/cellulose whiskers nanocomposites via
613 miniemulsion polymerization. *Journal of Applied Polymer Science*, 114, 2946-
614 2955.
615 Bettaieb, F., Khiari, R., Hassa, M.L., Belgacem, M.N., Bras, J., Dufresne, A., &
616 Mhenni, M.F. (2015). Preparation and characterization of new cellulose

617 nanocrystals from marine biomass *Posidonia oceanica*. *Industrial Crops Products*,
618 72, 175-182.
619 Boonterm, M., Sunyadeth, S., Dedpakdee, S., Athichalinthorn, P., Patcharaphun, S.,
620 Mungkung, R., & Techapiesancharoenkij, R. (2015). Characterization and
621 comparison of cellulose fiber extraction from rice straw by chemical treatment and
622 thermal stem explosion. *Journal of Cleaner Production*, 134, 592-599.
623 Borkotoky, S. S., Dhar, P., & Katiyar, V. (2018). Biodegradable poly (lactic
624 acid)/Cellulose nanocrystals (CNCs)composite microcellular foam: Effect of
625 nanofillers on foam cellularmorphology, thermal and wettability behaviour.
626 *International Journal of Biological Macromolecules*, 106, 433-446.
627 Bras, J., Hassan, M.L., Bruzesse, C., Hassan, E.A., El-Wakil, N.A., & Dufresne, A.
628 (2010). Mechanical barrier and biodegradability properties of bagasse cellulose
629 whiskers reinforced natural rubber nanocomposites. *Industrial Crops Products*, 32,
630 627-633.
631 Brigham, C. (2018). Biopolymers: biodegradable alternatives to traditional plastics. In:
632 B. Török, & T. Dransfield (Eds.), *Green Chemistry* (pp. 753-770). Amsterdam:
633 Elsevier Inc.
634 Brinchi, L., Cotana, F., Fortunati, E., & Kenny, J.M. (2013). Production of
635 nanocrystalline cellulose from lignocellulosic biomass: Technology and
636 applications. *Carbohydrate Polymers*, 94, 154-169.
637 Cano, A., Fortunati, E., Cháfer, M., González-Martínez, C., Chiralt, A., & Kenny, J. M.
638 (2015). Effect of cellulose nanocrystals on the properties of pea starch-poly(vinyl
639 alcohol) blend films. *Journal of Materials Science*, 50, 6979-6992.
640 Chauve, G., Fraschini, C., & Jean, B. (2013). Separation of cellulose nanocrystals. In
641 K. Oksman, A. P. Mathew, A. Bismark, O. Rojas, & M. Sain (Eds), *Handbook of*

642 *Green Materials: Processing Technologies, Properties and Applications* (pp. 73-
643 87). World Scientific Publishing Co.
644 Chen, W. S., Yu, H. P., Liu, Y. X., Chen, P., Zhang, M. X., & Hai, Y. F. (2011).
645 Individualization of cellulose nanofibers from wood using high-intensity
646 ultrasonication combined with chemical pretreatments. *Carbohydrate Polymers*,
647 83(4), 1804-1811.
648 Cherian, B. M., Leâo, A. L., de Souza, S. F., Costa, L. M. M., de Olyveira, G. M.,
649 Kottaisamy, M., Negarajan, E. R., & Thomas, S. (2011). Cellulose nanocomposites
650 with nanofibres isolated from pineapple leaf fibers for medical applications.
651 *Carbohydrate Polymers*, 86, 1790-1798.
652 El Achaby, M., Kassab, Z., Aboulkas, A., Gaillard, C., & Barakat, A. (2018). Reuse of
653 red algae waste for the production of cellulose nanocrystalsand its application in
654 polymer nanocomposites. *International Journal of Biological Macromolecules*,
655 106, 681-691.
656 Espino, E., Cakir, M., Domenek, S., Román-Gutiérrez, A. D., Belgacem, N., & Bras, J.
657 (2014). Isolation and characterization of cellulose nanocrystals from industrial by-
658 products of Agave tequilana and barley. *Industrial Crops Products*, 62, 552-559.
659 Fabra, M. J., López-Rubio, A., & Lagarón, J. M. (2014). Biopolymers for food
660 packaging applications. In M.R. Aguilar De Armas, & J.S. Román (Eds.), *Smart*
661 *Polymers and their Applications* (pp. 476-509). United Kingdom: Woodhead
662 Publishing.
663 Fahma, F., Iwamoto, S., Hori, N., Iwata, T., & Takemura, A. (2011). Effect of pre –
664 acid-hydrolysis treatment on morphology and properties of cellulose nanowhiskers
665 from coconut husk. *Cellulose*, 18, 443–450.

FAO. (2016). Food and Agriculture Organization of the United Nations (FAO). Rice Market Monitor, vol 11, No. 2. http://www.fao.org/ economic/est/publications/ rice-publications/rice-market-monitor-rmm/en/. (Accessed 27.04.2017).

Favier, V., Cavaille, J. Y., Canova, G. R., & Shrivastavas, S. C. (1997). Mechanical percolation in cellulose whisker nanocomposites. *Polymer Engineering and Science*, 37(10), 1732-1739.

Fengel, D., & Wegener, G. (1984). *Wood Chemistry, Ultrastructure, Reactions*. (1th ed.). New York: Walter de Gruyter, (Chapter 3).

Flauzino Neto, W. P., Silvério, H. A., Dantas, N. O., & Pasquini, D. (2013). Extraction and characterization of cellulose nanocrystals from agro-industrial residue soy hulls. *Industrial Crops Products*, 42, 480-488.

Fortunati, E., Puglia, D., Luzi, F., Santulli, C., Kenny, J. M., & Torre, L. (2013). Binary PVA bio-nanocomposites containing cellulose nanocrystals extracted from different natural sources: part I. *Carbohydrate Polymers*, 97, 825-836.

Fortunati, E., Luzi, F., Jiménez, A., Gopakumar, D. A., Puglia, D., Thomas, S., Kenny, J. M., Chiralt, A., & Torre, L. (2016). Revalorization of sunflowers stalks as novel sources of cellulose nanofibrils and nanocrystals and their effect on wheat gluten. *Carbohydrate Polymers*, 149, 357-368.

Ghanbarzadeh, B., Almasi, H., & Entezami, A. A. (2011). Improving the barrier and mechanical properties of corn starch-based edible films: Effect of citric acid and carboxymethyl cellulose. *Industrial Crops Products*, 33(1), 229-235.

González, K., Retegi, A., González, A., Eceiza, A. & Gabilondo, N. (2015). Starch and cellulose nanocrystals together into thermoplastic starch bionanocomposites. *Carbohydrate Polymers*, 117, 83-90

690 Habibi, Y., & Dufresne, A. (2008). Highly filled bionanocomposites from
691 functionalized polysaccharide nanocrystals. *Biomacromolecules*, 9, 1974-1980.
692 Hake, A., Mondal, D., Khan, I., Usmani, M. A., Bhat, A. H., & Gazal, U. (2017).
693 Fabrication of composites reinforced with lignocellulosic materials from
694 agricultural biomass. In: M. Jawaid, P. M. Tahir, & N. Saba (Eds.), *Lignocellulosic*
695 *fibre and biomass-based composite materials* (pp. 179-191). United Kingdom:
696 Woodhead Publishing.
697 Hassan, M. L., Mathew, A. P., Hassan, E. A., El-Wakil, N. A., & Oksman, K. (2012).
698 Nanofibers from bagasse and rice straw: process optimization and properties. *Wood*
699 *Science and Technology*, 46, 193-205.
700 Henrique, M. A., Silvério, H. A., Neto, W. P. F., & Pasquini, D. (2013). Valorization
701 of an agro-industrial waste, mango seed, by the extraction and characterization of
702 its cellulose nanocrystals. *Journal of Environmental Management*, 121, 202-209.
703 Hossain, A. B. M. S., Ibrahim, N. A., & AlEissa, M. S. (2016). Nano-cellulose derived
704 bioplastic biomaterial data for vehicle bio-bumper from banana peel waste biomass.
705 *Data in Brief, 8*, 286-294.
706 Jiang, L., & Zhang, J. (2017). Biodegradable and biobased polymers. In: M. Kutz
707 (Ed.), *Applied Plastics Engineering Handbook* (pp. 127-143). New York: William
708 Andrew.
709 Johar, N., Ahmad, I., & Dufresne, A. (2012). Extraction, preparation and
710 characterization of cellulose fibres and nanocrystals from rice husk. *Industrial*
711 *Crops Products*, 37, 93-99.
712 Jonoobi, M., Oladi, R., Davaoudpour, Y., Oksman, K., Dufresne, A., Hamzeh, Y., &
713 Davoodi, R. (2015). Different preparation methods and properties of nanostructured

cellulose from various natural resources and residues: a review. *Cellulose*, 22, 935-969.

Kallel, F., Bettaieb, F., Khiari, R., García, A., Bras, J., & Ellouz Chaabouni, S. (2016). Isolation and structural characterization of cellulose nanocrystals extracted from garlic straw. *Industrial Crops and Products*, 87, 287-296.

Kargarzadeh, H., Ahmad, I., Abdullah, I., Dufresne, A., Zainudin, S. Y., & Sheltami, R. M. (2012). Effects of hydrolysis conditions on the morphology, crystallinity, and thermal stability of cellulose nanocrystals extracted from kenaf bast fibers. *Cellulose*, 19, 855-866.

Kargarzadeh, H., Johar, N., & Ahmad, I. (2017). Starch biocomposite film reinforced by multiscale rice husk fiber. *Composite Science and Technology*, 15, 147-155.

Kaushik, M., Fraschini, C., Chauve, G., Putaux, J. L., & Moores, A. (2015). Transmission electron microscopy for the characterization of cellulose nanocrystals. In K. Maaz (Ed.), *The Transmission Electron Microscope - Theory and Applications* (pp. 129-163). InTech.

Khalil, H. P. S. A., Davoudpour, Y., Saurabh, C. K., Hossain, Md. S., Adnan, A. S., Dungani, R., Paridah, M. T., Sarker, Md. Z. I., Fazita, M. R. N., Syakir, M. I., & Haafiz, M. K. M. (2016). A review on nanocellulosic fibres as new material for sustainable packaging: Process and applications. *Renewable and Sustainable Energy Reviews*, 64, 823-836.

Khawas, P., & Deka, S. C. (2016). Isolation and characterization of cellulose nanofibers from culinary banana peel using high-intensity ultrasonication combined with chemical treatment. *Carbohydrate Polymers*, 137, 608-616.

Le Normand, M., Moriana, R., & Ek, M. (2014). Isolation and characterization of cellulose nanocrystals from spruce bark in a biorefinery perspective. *Carbohydrate Polymers*, 111, 979-987.

Li, R., Fei, J., Cai, Y., Li, Y., Feng, J., & Yao, J. (2009). Cellulose whiskers extracted from mulberry: a novel biomass production. *Carbohydrate Polymers*, 76, 94–99.

Lima, M. M. S., & Borsali, R. (2004). Rod-like cellulose microcrystal: structure, properties, and applications. *Macromolecular Rapid Communication*, 25, 771–787.

Ludueña, L., Vázquez, A., & Alvarez, V. (2012). Effect of lignocellulosic filler type and content on the behavior of polycaprolactone based eco-composites for packaging applications. *Carbohydrate Polymers*, 87, 411-421.

Luzi, F., Fortunati, E., Jiménez, A., Puglia, D., Pezzolla, D., Gigliotti, G., Kenny, J. M., Chiralt, A., & Torre, L. (2016). Production and characterization of PLA_PBS biodegradable blends reinforced with nanocrystals extracted from hemp fibres. *Industrial Crops and Products*, 93, 276-289.

Mansaray, K. G., & Ghaly, A. E. (1998). Thermal degradation of rice husks in nitrogen atmosphere. *Bioresource Technology*, 65, 13-20.

Mondal, S. (2017). Preparation, properties and applications of nanocellulosic materials. *Carbohydrate Polymers,* 163, 301-316.

Moreno-Contreras, G. G., Serrano-Rico, J. C., & Palacios-Restrepo, J. A. (2009). Industrial waste combustion performance in a bubbling fluidized bed reactor. *Ingeniería Universidad de Bogotá,* 13, 251-266.

Moriana, R., Vilaplana, F., & Ek, M. (2016). Cellulose nanocrystals from forest residues as reinforcing agents for composites: a study from macro- to nano-dimensions. *Carbohydrate Polymers*, 139, 139-149.

National Renewable Energy Laboratory, NREL/TP-510-42618., 2011. Determination of structural carbohydrates and lignin in biomass. Colorado.

National Renewable Energy Laboratory, NREL/TP-510-42619., 2008. Determination of extractives in biomass. Colorado.

Ng, H. M., Sin, L. T., Tee T. T., Bee S. T., Hui, D., Low, C. Y., & Rahmat, A. R. (2015). Extraction of cellulose nanocrystals from plant sources for application as reinforcing agent in polymers. *Composites Part B*, 75, 176-200.

Ni, Y., Kubes, G. J., & Van Helnlngen, A. R. P. (1993). Mechanism of chlorate formation during bleaching of kraft pulp with chlorine dioxide. *Pulp Paper Science*, 19, 1-5.

Oliveira, L. S., Franca, A. S. (2016). An overview of the potential uses for coffee husks. *Coffee in Health Disease and Prevention*, 31, 283-291.

Ortega-Toro, R., Santagata, G., Gomez D'Ayala, G., Cerruti, P., Talens Oliag, P., Chiralt Boix, M.A., & Malinconico, M. (2016a). Enhancement of interfacial adhesion between starch and grafted poly(-caprolactone). *Carbohydrate Polymers*, 147, 16-27.

Ortega-Toro, R., Collazo-Bigliardi, S., Talens, P., & Chiralt, A. (2016b). Thermoplastic starch: improving their barrier properties. *Agronomía Colombiana*, 34, 73-75.

Patel, J. P., & Parsania, P. H. (2018). Characterization, testing, and reinforcing materials of biodegradable composites. In: N. G. Shimpi (Ed.), *Biodegradable and Biocompatible Polymer Composites* (pp. 55-79). United Kingdom: Woodhead Publishing.

Qiao, C., Chen, G., Zhang, J., & Yao, J. (2016). Structure and rheological properties of cellulose nanocrystals suspension. *Food Hydrocolloids*, 55, 19-25.

Reddy, J. P., & Rhim, J. W. (2014). Isolation and characterization of cellulose nanocrystals from garlic skin. *Materials Letters*, 129, 20-23

Reis, K. C., Pereira, L., Nogueira Alves Melo, I. C., Marconcini, J. M., Trugilho, P. F., & Denzin Tonoli, G. H. (2015). Particles of coffee wastes as reinforcement in polyhydroxybutyrate (PHB) based composites. *Materials Research*, 18 (3), 546-552.

Roman, M., & Winter, W. T. (2004). Effect of sulfate groups from sulfuric acid hydrolysis on the thermal degradation behavior of bacterial cellulose. *Biomacromolecules*, 5, 1671–1677.

Rosa, M. F., Medeiros, E. S., Malmonge, J. A., Gregorski, K. S., Wood, D. F., & Mattoso, L. H. C. (2010). Cellulose nanowhiskers from coconut husk fibers: effect of preparation conditions on their thermal and morphological behavior. *Carbohydrate Polymers*, 81, 83-92.

Sanjay, M. R., Madhu, P., Jawaid, M., Senthamaraikannan, P., Senthil, S., & Pradeep, S. (2018). Characterization and properties of natural fiber polymer composites: A comprehensive review. *Journal of Cleaner Production*, 172, 566-581.

Santos, R. P. O., Rodrigues, B. V. M., Ramires, E. C., Ruvolo-Filho, A. C., & Frollini, E. (2015). Bio-based materials from the electrospinning of lignocellulosic sisal fibers and recycled PET. *Industrial Crops and Products*, 72, 69-76.

Savadekar, N. M., & Mhaske, S. T. (2012). Synthesis of nano cellulose fibers and effect on thermoplastics starch based films. *Carbohydrate Polymers*, 89, 146-151.

Shebani, A. N., van Reenen, A. J., & Meincken, M. (2008). The effect of wood extractives on the thermal stability of different wood species. *Thermochimica Acta*, 471, 43-50.

Sheltami, R. M., Abdullah, I., Ahmad, I., Dufresne, A., & Kargarzadeh, H. (2012). Extraction of cellulose nanocrystals from Mengkuang leaves (Pandanus tectorius). *Carbohydrate Polymers*, 88, 772-779.

Shih, Y. F., Chang, W. C., Liu, W.C., Lee, C. C., Kuan, C. S., & Yu, Y. H. (2014). Pineapple leaf/recycled disposable chopstick hybrid fiber-reinforced biodegradable composites. *Journal of Taiwan Institute of Chemical Engineering*, 45(4), 2039-2046.

Slavustky, A. M., & Bertuzzi, M. A. (2014). Water barrier properties of starch films reinforced with cellulose nanocrystals obtained from sugarcane bagasse. *Carbohydrate Polymers*, 110, 53-61.

Silvério, H. A., Neto, W. P. F., Dantas, N. O., & Pasquini, D. (2013). Extraction and characterization of cellulose nanocrystals from corncob for application as reinforcing agent in nanocomposites. *Industrial Crops and Products*, 44, 427-436.

Singh, R., Shukla, A., Tiwari, S., & Srivastava, M. (2014). A review on delignification of lignocellulosic biomass for enhancement of ethanol production potential. *Renewable and Sustainable Energy Reviews*, 32, 713-728.

Siqueira, G., Bras, J., & Dufresne, A. (2010). Cellulosic bionanocomposites: a review of preparation, properties and applications. *Polymer*, 2, 728-765.

Sundari, M. T., & Ramesh, A. (2012). Isolation and characterization of cellulose nanofibers from the aquatic weed water hyacinth—*Eichhornia crassipes*. *Carbohydrate Polymers*, 87, 1701-1705.

Talegaonkar, S., Sharma, H., Pandey, S., Mishra, P. K., & Wimmer, R. (2017). Bionanocomposites: smart biodegradable packaging material for food preservation. In: A. M. Grumezescu (Ed.), *Food Packaging* (pp. 79-110). Cambridge: Academic Press.

835 Zainuddin, S. Y. Z., Ahmad, I., Kargarzadeh, H., Abdullah, I., & Dufresne, A. (2013).
836 Potential of using multiscale kenaf fibers as reinforcing filler in cassava starch-
837 kenaf biocomposites. *Carbohydrate Polymer*, 92, 2299-2305.